Structural Eng./Earthquake Eng., JSCE, Vol. 18, No. 1, 41s—52s, 2001 April
(J. Struct. Mech. Earthquake Eng., JSCE, No. 675/ I —55)

LARGE DEFORMATION BEHAVIOR OF BURIED PIPELINES WITH LOW-ANGLE ELBOWS SUBJECTED TO PERMANENT GROUND DEFORMATION

Koji YOSHIZAKI[1], Thomas D. O'ROURKE[2] and Masanori HAMADA[3]

[1]Member of JSCE, M. Eng., Research Engineer, Fundamental Technology Laboratory, Tokyo Gas
(1-16-25, Shibaura, Minato-ku, Tokyo 105-0023, Japan)
[2]Member of ASCE, Ph. D., Professor, School of Civil and Environmental Eng., Cornell University
(Hollister Hall, Ithaca, NY 14853, USA)
[3]Fellow of JSCE, Dr. Eng., Professor, Dept. of Civil Eng., Waseda University
(3-4-1, Okubo, Shinjuku-ku, Tokyo 169-8555, Japan)

Substantial permanent ground deformation (PGD) can be generated during earthquakes, causing deformation and strain that concentrates at pipeline elbows. This paper describes in-plane bending experiments on various kinds of low-angle elbows in the closing and opening mode, and Finite Element (FE) modeling to simulate their deformation behavior using linear shell elements. Good agreement was obtained between the analytical and experimental results, even for plastic deformation as much as 30% strain. Analytical results obtained with a modeling technique named HYBRID MODEL are also presented for the behavior of 300-mm-diameter buried pipelines with low-angle elbows subjected to PGD.

Key Words: *pipeline, low-angle elbow, earthquakes, gas utilities, experiment, FEM, ground deformation, liquefaction, landslides, lifelines*

1. INTRODUCTION

During earthquakes, permanent ground deformation (PGD) can damage buried pipelines. There is substantial evidence from previous earthquakes, such as the 1983 Nihonkai-Chubu[1)], the 1994 Northridge[2)], and the 1995 Hyogoken-Nanbu[3)] earthquakes, of gas pipeline damage caused by earthquake-induced PGD in the form of liquefaction and landslides. Because elbows represent locations of local restraint with respect to flexural and axial deformation of buried pipelines, strains can easily accumulate at elbows in response to PGD.

Yoshizaki et al.[4), 5)] have shown a favorable comparison between the results of in-plane bending experiments with 90° elbows and the analytical results of Finite Element (FE) modeling for strains as high as 25%. In the field, however, many elbows are installed with angles less than 90°, and damage to these facilities has been observed during past earthquakes. Moreover, the large deformation behavior of low-angle elbows has received only limited coverage in previous papers[6),7)] and guidelines for earthquake-resistant design of gas pipelines[8), 9)].

Gas pipeline companies should be able to maintain their buried pipelines without leakage even if the lines are subjected to large deformation during earthquakes. Therefore, it is important to clarify the deformation behavior of buried pipelines with low-angle elbows up to their limit state against large ground deformation.

The purpose of this paper is to present experimental results and an analytical method for assessing the behavior of buried pipelines with low-angle elbows subjected to very high levels of strain. In-plane bending experiments were conducted in the closing and opening mode for various kinds of elbows until the measured strain exceeded 30%. Finite Element (FE) modeling was also performed to represent the deformation behavior of the elbows. Furthermore, a modeling technique named HYBRID MODEL, which was developed for simulating the effects of PGD on buried pipelines with elbows in the previous

papers[4), 5)], was applied to pipelines with low-angle elbows. In this paper analytical results obtained with this model are presented for the behavior of 300-mm-diameter buried pipelines with low-angle elbows subjected to PGD.

2. BENDING EXPERIMENTS OF LOW-ANGLE PIPELINE ELBOWS

(1) Experimental method

In-plane bending experiments were carried out in the closing and opening mode for pipeline elbows with different geometric characteristics. The experiments involved pipe specimens with 100, 200 and 300-mm diameters and initial bend angles of 45°, 22.5° and 11.25°. The radius of curvature was 1.5 times the diameter. The elbows were composed of STPT 370 steel (Japanese Industrial Standard, JIS-G3456), with a specified minimum yield stress of 215 MPa and a minimum ultimate tensile strength of 370 MPa. The straight pipe was composed of SGP steel (JIS-G3452), with a minimum ultimate tensile strength of 294 MPa. The dimensions of the test pipes are presented in **Table 1**. In this table, the outside diameter is the average of the measured values of the specimen.

The elbows were fabricated with mandrels at elevated temperatures. Pipe wall thickness was measured with an ultrasonic meter at ten-degree increments in the circumferential direction. The thicknesses listed in **Table 1** are the means of all specimens with the same diameter. Variations in wall thickness were typically within ±20% with respect to the mean.

Fig. 1 illustrates the experimental setup and the definition of the "closing" and "opening" mode. Straight pipes with lengths of about 2.5 times the diameter for 200-mm and 300-mm-diameter pipes and 5 times the diameter for 100-mm-diameter pipes were welded to each end of the test elbows. The length of the straight pipes was determined so that we could conduct the experiment until the both ends of the specimen came into contact in the closing mode. The I-beam used in the setup was selected to be much stiffer than the pipe specimen. Displacement was applied with a hydraulic jack in one direction with displacement control for both the closing and opening mode. Because it has already been confirmed by Minami et al.[10] and Yoshizaki and Oguchi[11] that strain rate due to seismic motion has little influence on the stress-strain relationship of gas pipeline steel, the displacement was applied with 1 mm/sec approximately. Internal pressure of 0.1 MPa was added with nitrogen. The test was stopped if the both ends of the specimen came into contact with each other in the closing mode, a maximum load of 490 kN was attained, or leakage occurred.

Table 1 Summary of experimental pipe dimensions

Nominal diameter (mm)		100	200	300
Elbow	Outside diameter, Do (mm)	116.5	218.4	319.9
	Pipe thickness, t (mm)	5.4	6.8	7.4
	Do/t	21	32	43
Straight pipe	Wall thickness, t (mm)	4.1	5.2	6.5

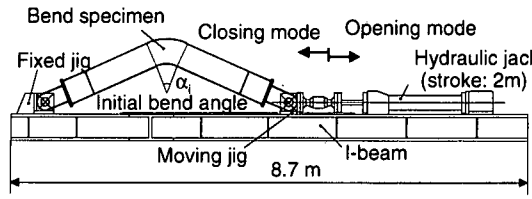

Fig. 1 Experimental setup

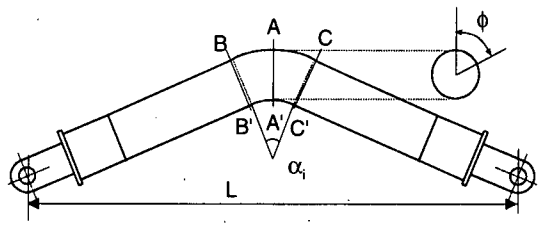

Fig. 2 Strain gauge locations

Test data were obtained with a load cell, displacement meter, pressure gauge, and strain gauges that were bonded in the circumferential and longitudinal directions on the external pipe surface at the three cross-sections illustrated in **Fig. 2**. The gauge length of the strain gauges was 5 mm. As many as 150 strain gauges were used in each test set-up. During each experiment, the acquisition of strain measurements at a given location was continued by replacing the gauges which reached their strain limit of 10% with new gauges at the same location. In addition, changes in the deformed shape of the external pipe surface of the A-A' section illustrated in **Fig. 2** (hereafter, "the central cross-section") were measured intermittently with a 3-dimentional displacement measuring device, employing five arms with five encoders.

(2) Discussion of experimental results

Table 2 summarizes the experimental maximum strain, direction of maximum strain, maximum change in bend angle, and observations pertaining to leakage in combination with the results of the previous experiments on 90° elbows[4), 5)]. In this

Table 2 Summary of test results

Initial bend angle, α_i		Nominal Diameter	100-mm	200-mm	300-mm
Closing mode	90°	Maximum strain, ε_{max}	25%, Circum.	30%, Circum.	25%, Circum.
		Max bend angle change, $\Delta\alpha_{max}$	78°	86°	81°
		Presence of leakage	No	No	No
	45°	Maximum strain, ε_{max}	32%, Long.	53%, Long.	43%, Long.
		Max bend angle change, $\Delta\alpha_{max}$	119°	118°	113°
		Presence of leakage	No	No	No
	22.5°	Maximum strain, ε_{max}	57%, Long.	41%, Circum.	72%, Long.
		Max bend angle change, $\Delta\alpha_{max}$	133°	134°	134°
		Presence of leakage	No	No	No
	11.25°	Maximum strain, ε_{max}	58%, Long.	53%, Long.	0.1%, Circum.
		Max bend angle change, $\Delta\alpha_{max}$	150°	145°	6°
		Presence of leakage	No	No	(Load limit)
Opening mode	90°	Maximum strain, ε_{max}	40%, Long.	42%, Long.	33%, Circum.
		Max bend angle change, $\Delta\alpha_{max}$	-44°	-33°	-44°
		Presence of leakage	Yes	Yes	(Load limit)
	45°	Maximum strain, ε_{max}	31%, Long.	22%†, Long.	3%, Circum.
		Max bend angle change, $\Delta\alpha_{max}$	-45°‡	-23°	-8°
		Presence of leakage	Yes	Yes	(Load limit)
	22.5°	Maximum strain, ε_{max}	13%†, Long.	9%, Long.	0.7%, Circum.
		Max bend angle change, $\Delta\alpha_{max}$	-22°‡	-10°	-4°
		Presence of leakage	Yes	(Load limit)	(Load limit)
	11.25°	Maximum strain, ε_{max}	9%, Long.	3%, Long.	—
		Max bend angle change, $\Delta\alpha_{max}$	-11°‡	-11°‡	—
		Presence of leakage	(Load limit)	(Load limit)	—

Circum.: Circumferential, Long.: Longitudinal †: Maximum strain could not be measured.
‡: Maximum bend angle change at full extension of elbow (see **Fig. 2**)

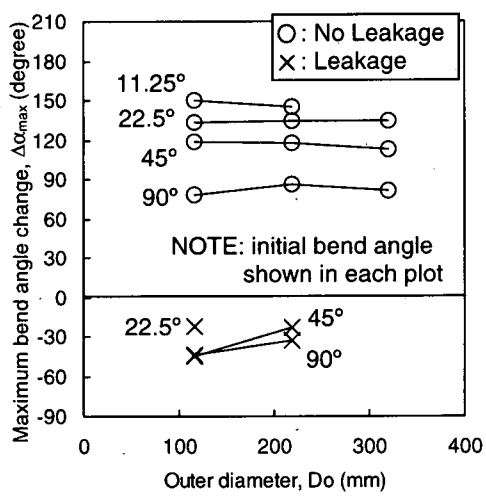

Fig. 3 Maximum changes in bend angle during tests

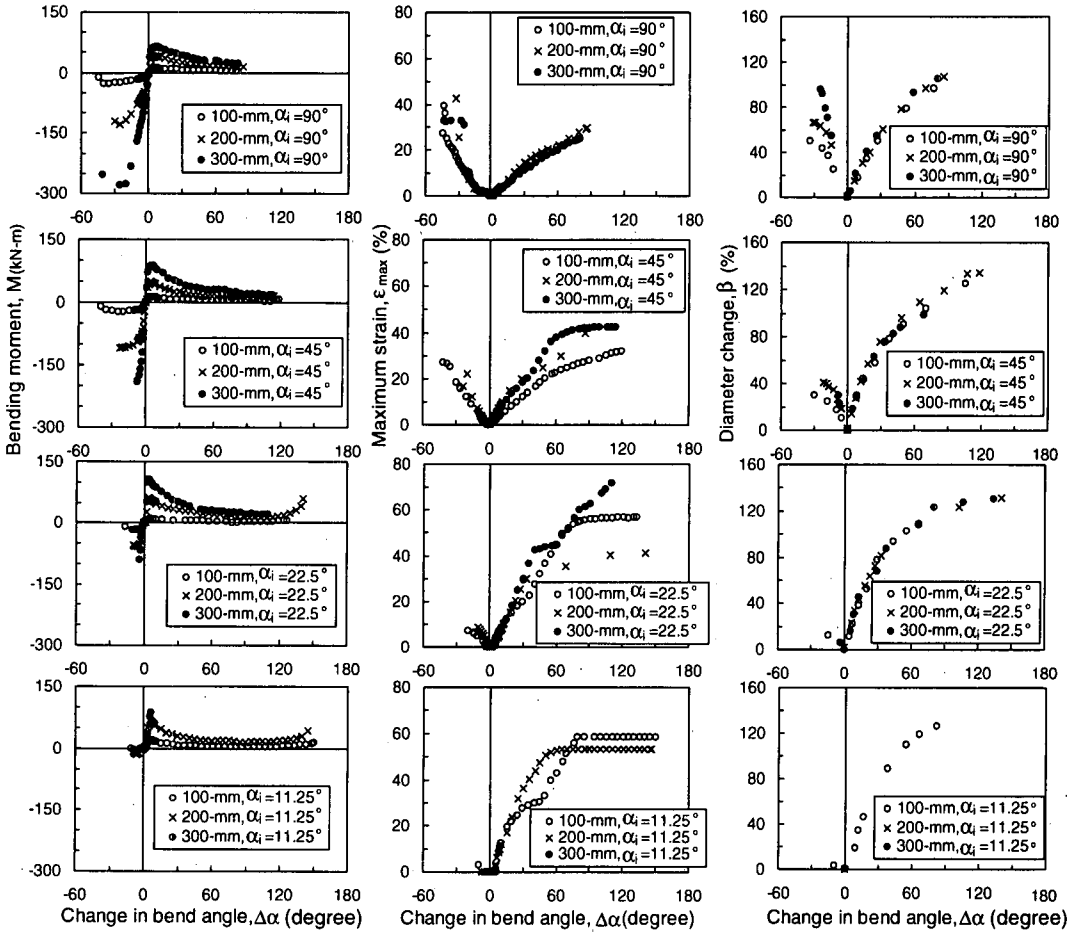

(a) Bending moment (b) Maximum strain (c) Diameter change

Fig. 4 Results of bending experiments

table, maximum strain means the maximum value of all circumferential and longitudinal strains measured with strain gauges, and is expressed as positive if it is tensile and negative if compressive. For the 100-mm elbow with 22.5° of initial bend angle and the 200-mm elbow with 45° of initial bend angle, maximum strain could not be measured because cracking occurred at a location somewhat distant from the nearest gauges. The change in bend angle $\Delta\alpha$ in this table was calculated with the following formula on the assumption that the specimen is a triangle:

$$\Delta\alpha = 2\cdot\cos^{-1}\left(\frac{L-\delta}{L}\cos\frac{\alpha_i}{2}\right)-\alpha_i \qquad (1)$$

In this formula, L, δ and α_i are the initial distance between the ends of the specimen (illustrated in **Fig. 2**), displacement of the jack, and initial bend angle, respectively. **Fig. 3** summarizes the maximum change in bend angle that was caused without exceeding the load limit of the hydraulic jack.

Fig. 4 shows (a) bending moment, (b) maximum strain, (c) diameter change vs. change in bend angle. Here, the maximum strain represents the maximum of the absolute values of all measured strains. Bending moment, M, and diameter change, β, are calculated with the following formulas:

$$M = F\cdot\sqrt{\left(\frac{L}{2\cos\frac{\alpha_i}{2}}\right)^2-\left(\frac{L-\delta}{2}\right)^2} \qquad (2)$$

$$\beta = \frac{D_{max}-D_{min}}{\overline{D}_0}\times 100 \qquad (3)$$

In these formulas, F, D_{max}, D_{min}, and $\overline{D}_0$ are, respectively, reaction force measured by a load cell between the jack and the specimen, longest diameter (major axis) of the deformed central cross-section, its shortest diameter (minor axis), and the

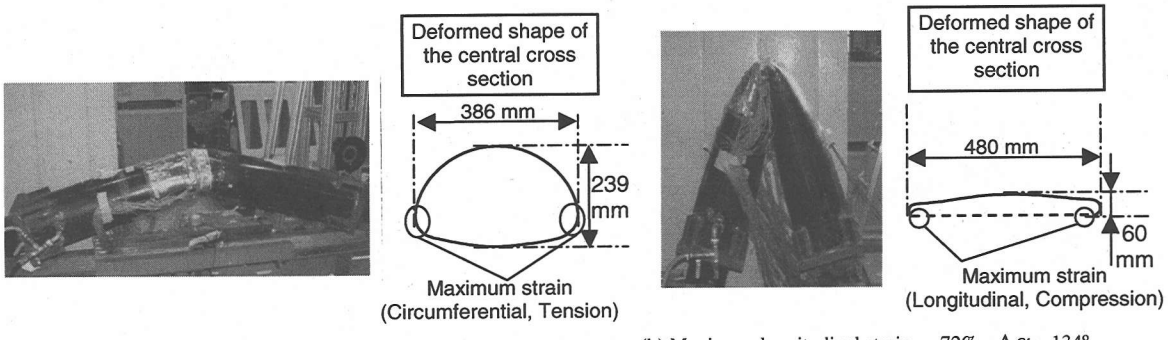

(a) Maximum circumferential strain = 10%, $\Delta\alpha$ = 12°

(b) Maximum longitudinal strain = -72%, $\Delta\alpha$ = 134°

Fig. 5 Longitudinal and transverse deformation of a 300-mm-diameter elbow with 22.5° of initial bend angle in the closing mode

average of the initial diameter of the undeformed central cross-section.

The deformation behavior was different in the closing and opening mode. In the closing mode, no leakage occurred even when both straight pipes connected to the elbow came into contact with each other and the measured maximum strain exceeded 70%. Elbows with smaller initial bend angles experienced larger changes of bend angle, as indicated in **Fig. 3**.

Fig. 5 shows deformation in the closing mode and the deformed shape of the central cross-section of a 300-mm elbow with 22.5° of initial bend angle. The deformation involved ovalization of the elbow. A maximum circumferential tensile strain of 10% was measured when the change in bend angle, $\Delta\alpha$, was 12° (see **Fig. 5** (a)). Further increases in $\Delta\alpha$ resulted in a shift of maximum strain from circumferential tension to longitudinal compression. A maximum longitudinal compressive strain of 74% was measured at ϕ = 120° (see **Fig. 2**) when $\Delta\alpha$=134° (see **Fig. 5** (b)). Because of difficulties in locating and replacing strain gauges at the precise locations of high deformation and curvature, it is likely that the actual maximum strains were larger than those measured with strain gauges and plotted in the figure. The deformed shape is also interpolated with dotted line in **Fig. 5** (b) because of difficulty in locating the displacement measuring device.

For the pipes, which had same initial bend angle, elbows with larger diameters had larger bending moments for a given change in bend angle, as shown in **Fig. 4** (a) in the closing mode. Pipe diameter, however, had little effect on the relationships between both maximum strain and diameter change and changes in the bend angle, as shown in **Fig. 4** (b) and (c), respectively. For the same diameter pipes, elbows with smaller initial

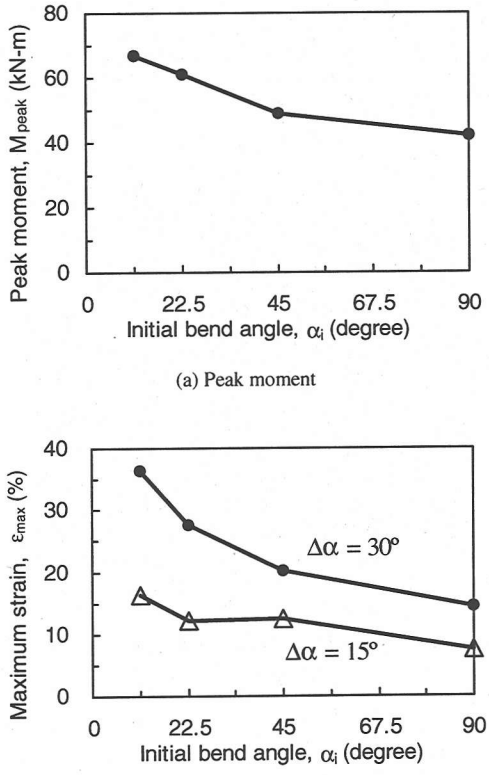

(a) Peak moment

(b) Maximum strain

Fig. 6 Deformation behavior in the closing mode of 200-mm-diameter elbows with various initial bend angles

bend angles had larger peak values of moment and tended to have larger maximum strains for the same change in bend angle, as plotted in **Fig. 6** (a) and (b), respectively. There is a significant decrease in maximum strain as a function of initial bend angle for $\Delta\alpha$ = 30° shown in **Fig. 6** (b), and a more moderate decrease for $\Delta\alpha$ = 15°. The main reason for this behavior is that elbows with smaller initial

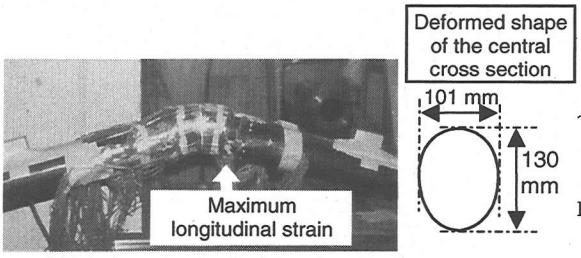

(a) Maximum longitudinal strain = 10%, $\Delta\alpha$ = -24°

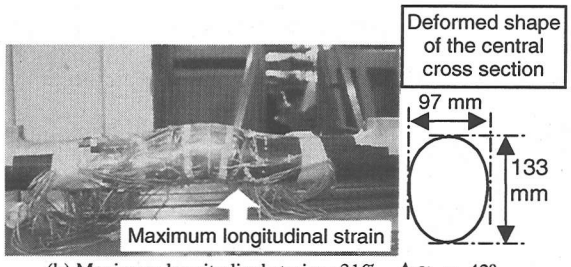

(b) Maximum longitudinal strain = 31%, $\Delta\alpha$ = -42°

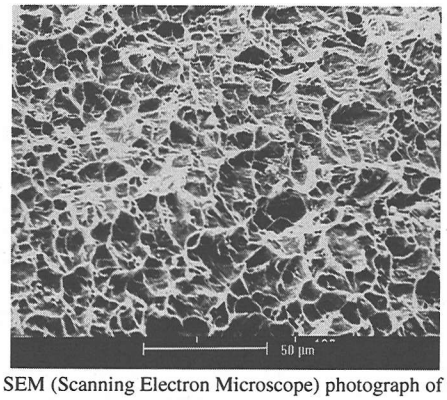

(c) SEM (Scanning Electron Microscope) photograph of the fractured surface

Fig. 7 Longitudinal and transverse deformation and SEM photograph of the fractured surface of a 100-mm-diameter elbow with 45° of initial bend angle in the opening mode

bend angles experience greater localized deformation, which is similar to the buckling behavior of a straight pipe subjected to combined compression and bending.

Leakage was observed in the opening mode for all cases except the ones at the load limit of the hydraulic jack. **Fig. 7** shows the deformation behavior and the deformed shape of the central cross-section of a 100-mm elbow with 45° of initial bend angle. In contrast with the closing mode, ovalization during the opening mode was accompanied by increases in vertical diameter at the central cross-section (see **Fig. 7** (a) and (b)). In response to this change in the central cross-section shape, the stiffness of the elbow became larger than that of the straight pipe. Bending was then

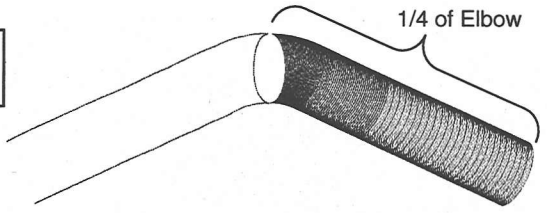

Fig. 8 Finite Element model for 300-mm-diameter elbow with 45° of initial bend angle

concentrated at the location where one of the straight pipes was connected to the elbow. In all cases, leakage occurred near a straight pipe girth weld at ϕ = 180°.

The deformed shapes of the central cross-section are illustrated in **Fig. 7** (a) and (b). The maximum strains, however, were located near the welds connecting the straight pipes to the elbow. The maximum longitudinal strain locations are indicated in photos of the deformed test specimen in **Fig. 7** (a) and (b). The maximum strain measured near the crack was 31% in the longitudinal direction. Necking was observed in the pipe metal outside the heat-affected zone, but close to the crack. **Fig. 7** (c) is a SEM (Scanning Electron Microscope) photograph of the fracture surface of the 100-mm-diameter elbow that indicates a ductile fracture.

Compared with the closing mode, the maximum changes in bend angle were much smaller, as shown in **Fig. 3**. For the pipes that had the same initial bend angle, elbows with larger diameters sustained larger bending moments, larger maximum strains, and larger diameter changes for the same change in bend angle, as shown in **Fig. 4** (a), (b) and (c), respectively.

3. FINITE ELEMENT ANALYSES FOR LOW-ANGLE PIPELINE ELBOWS

(1) Analytical model

Finite element analyses were performed to study the deformation behavior of the low angle elbows. **Fig. 8** shows the FE model for the 300-mm diameter pipe with 45° of initial bend angle. Because of symmetry, only a quarter of the specimen was modeled, for which half the pipe circumference was analyzed. The elements used in the model are isotropic linear shell elements with reduced integration points, which consider shear deformation. Seventy-two elements were employed around half the pipe circumference. The aspect ratio for elbows and straight pipe near the elbow was 1:1 and that for the other straight pipe was 1:5, as shown in **Fig. 8**. The total number of elements was

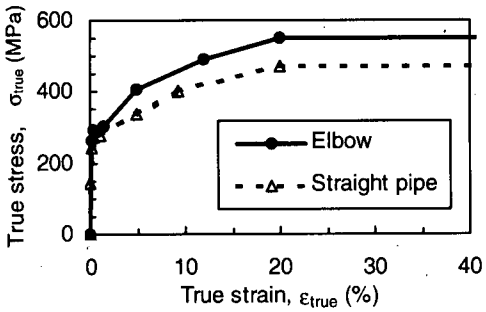

Fig. 9 Stress-strain curves used in FE modeling

Table 3 Mechanical properties used in FE Analysis

	Elbow	Straight pipe
Young's modulus, E (GPa)	206	206
Poisson's ratio, ν	0.3	0.3
Yield stress, σ_y (MPa)	294	270
Tensile strength, σ_t (MPa)	451	385

about 7500, of which 4500 were concentrated near the center of the elbow.

The average value of the actual thickness measured with an ultrasonic thickness meter was used in the analytical model. The stress-strain relationship from tension test data was approximated by a multi-linear trend as plotted in **Fig. 9**. In the relationship between true stress and true strain, stress doesn't have a peak value. The modulus remains positive even as the engineering stress (ratio of force to original area) declines in response to reduced cross-sectional area due to necking. However, shell elements are not able to simulate necking, and they produce higher load if they retain a positive stiffness after the peak engineering stress[12]. Therefore, the relationships in **Fig. 9** were adjusted to show constant true stress when the true strain exceeds 20%. ABAQUS Version 5.8 was used as a solver for the analyses with geometric nonlinearity and large strain formulation. The von Mises criterion and associated flow rule were applied to the model. Since the straining is in the same direction in strain space throughout the analyses, isotropic hardening was also applied to the model[14].

(2) Analytical results and discussions

Fig. 10 compares the experimental and FE analytical results for the 300-mm elbows with 45° of initial bend angle. Good agreement exists between the experimental and analytical results with respect to the bending moments and maximum strains. The numerical modeling technique was able to simulate plastic strains as much as 40%, as shown in **Fig. 10** (c). The reason for the difference in maximum compressive strain between the experimental and FE analytical results for changes in bend angle

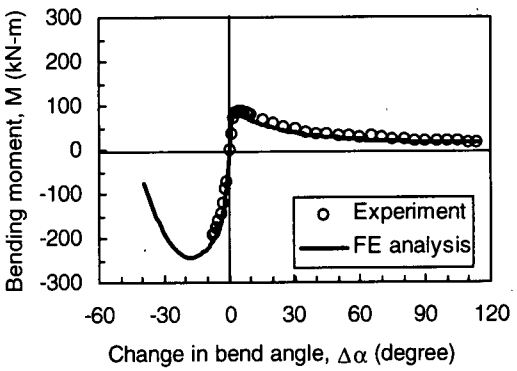

(a) Bending moment versus change in bend angle

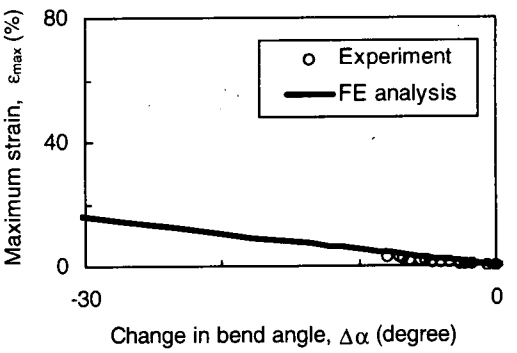

(b) Maximum strain versus change in bend angle (opening mode)

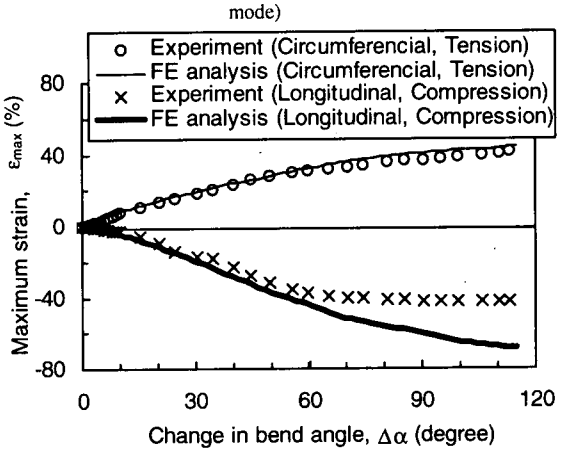

(c) Maximum strain versus change in bend angle (closing mode)

Fig. 10 Comparison between experiment and FE analyses for a 300-mm-diameter elbow with 45° of initial bend angle

above 60° (see **Fig. 10** (c)) is related to measurement limitations affected by difficulties in locating and replacing strain gauges at high deformation and curvature.

Fig. 11 (a) and (b) compare the analytical results with experimental ones for 300-mm elbows with 45° of initial bend angle when the change of bend angle was 110° in the closing mode. Good

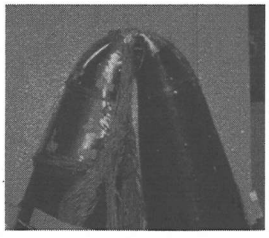

(a) Deformed shape (Experiment)

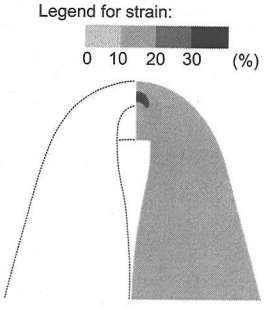

(b) Deformed shape and strain distribution (FE analysis)

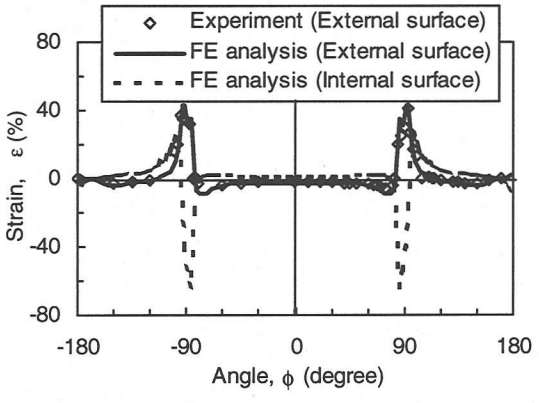

(c) Strain distribution in the circumferential direction

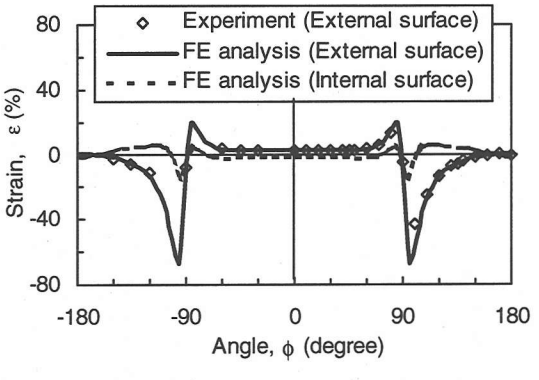

(d) Strain distribution in the longitudinal direction

Fig. 11 Deformed shape and strain distribution at the central cross-section of a 300-mm-diameter elbow with 45° of initial bend angle in the closing mode ($\Delta\alpha$ = 110°)

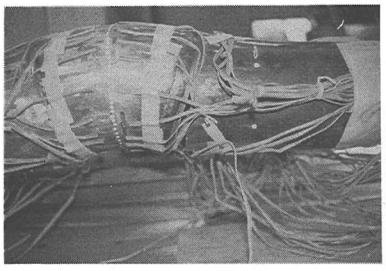

(a) Deformed shape (Experiment)

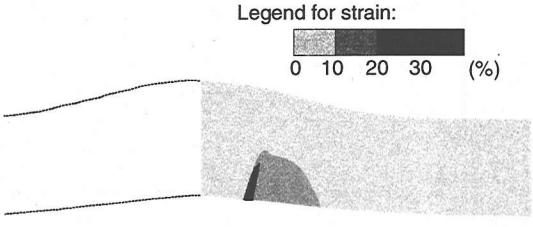

(b) Deformed shape and strain distribution (FE analysis)

Fig. 12 Deformed shape of a 100-mm-diameter elbow with 45° of initial bend angle in the opening mode ($\Delta\alpha$ = -45°)

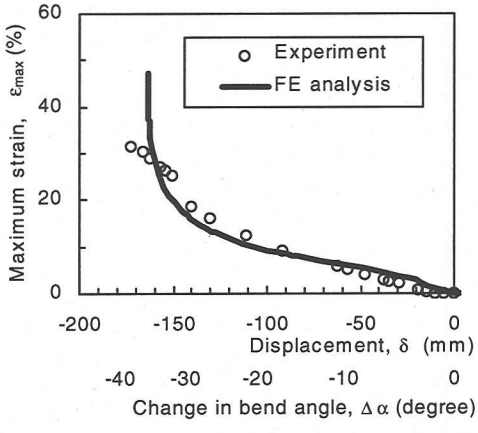

Fig. 13 Comparison between experiment and FE analysis for a 100-mm-diameter elbow with 45° of initial bend angle in the opening mode

agreement between experimental and analytical results was observed for strain distribution around the central cross-section in both the circumferential and longitudinal directions, as shown in **Fig. 11** (c) and (d), respectively. **Fig. 11** (c) and (d) also show the symmetry of strain values obtained in the experimental results in the circumferential direction.

Fig. 12 (a) and (b) compare the analytical and experimental results for a 100-mm elbow with 45° of initial bend angle when the change in bend angle was -45° in the opening mode. In the experiment, leakage occurred around one of the girth welds between the elbow and the straight pipes. In the welding process, it is not possible to make a perfectly symmetric specimen, which is assumed in the FE analytical model. The leakage occurs at locations of concentrated strain near the welds, which are represented in the FE analysis. As shown in **Fig. 13**, the model was able to simulate plastic strains as much as 30%.

4. ANALYSES OF BURIED PIPELINES WITH LOW-ANGLE ELBOWS SUBJECTED TO PGD

A modeling technique named HYBRID MODEL was developed for simulating large-scale pipeline and elbow response to PGD in the previous work[4),5),15)]. The model uses shell elements for the elbow and its neighboring part where large, localized strains occur. As shown in **Fig. 14** (a), the shell elements are located over a distance equal to 40 times the diameter from the center point of the elbow. The shell elements are linked to beam elements that extend beyond the distance of 20 times the diameter. Continuity of deformation between the shell and beam elements is enforced by the use of Multi-Point Constraint in ABAQUS[14)], as shown in **Fig. 14** (b). In this paper, analytical results for the behavior of 300-mm-diameter buried pipelines with various types of low-angle elbows, carrying 0.1 MPa internal pressure, are presented for plastic strains as high as 30%, using the material properties summarized in **Fig. 9** and **Table 3**.

Fig. 15 shows the assumed distribution of PGD. The direction of movement is shown by the large arrow, which is oriented at an angle, ψ, with respect to the elbow. In the x-direction (direction of movement), a triangular pattern of increasing and decreasing displacement was modeled. As shown in the figure, this pattern produces a zone of tensile and compressive ground strain. In the y-direction (perpendicular to movement direction), the displacements were distributed in a triangular pattern, with maximum movement at the apex of the equilateral triangle. This distribution of movement over a distance of 400 m is based on the model proposed by Hamada et al.[16)] and Satoh et al. [17)]

In the previous work[4), 5)], it was shown that severe deformation was caused when the elbow was positioned at the location of large displacement

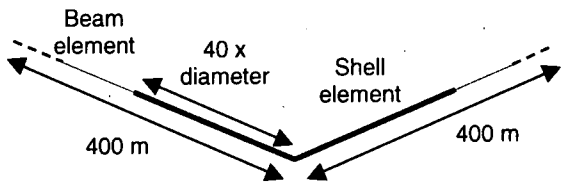

(a) Analytical model around elbow

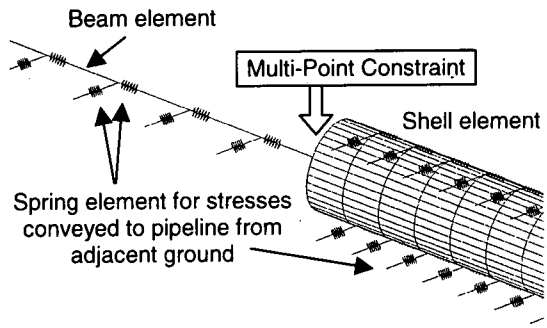

(b) Modeling for connection between shell elements and beam elements

Fig. 14 HYBRID MODEL used for analyses of buried pipelines

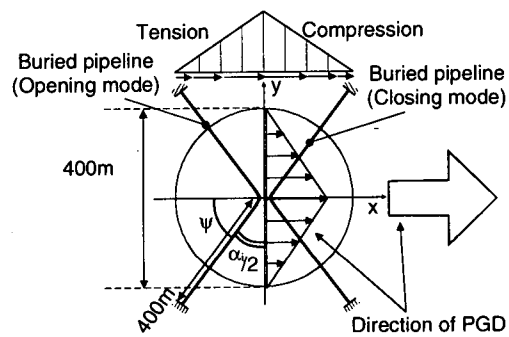

Fig. 15 Assumed model of PGD

regardless of ground strain or shape of PGD. Strain was also largest when ψ, the relative angle between the PGD direction and pipeline, was equal to 45° and 225° for elbows with 90° of initial bend angle in the opening and closing mode, respectively. Therefore, for each pipeline elbow with an initial bend angle of α_i, that was positioned at the locations of maximum displacement, an opening and closing mode case was analyzed with the parameter of ψ equal to $90°-\alpha_i/2$ and $90°+\alpha_i/2$, respectively (see **Fig. 15**).

The stresses conveyed to the pipeline from the adjacent ground were represented as stresses parallel and normal to the pipe longitudinal axis in accordance with the "Recommended Practice for

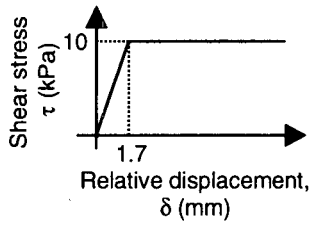

(a) Parallel to the pipe longitudinal axis[8)]

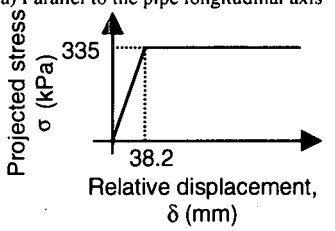

(b) Normal to the pipe longitudinal axis[18)]

Fig. 16 Stresses conveyed to pipeline from adjacent ground

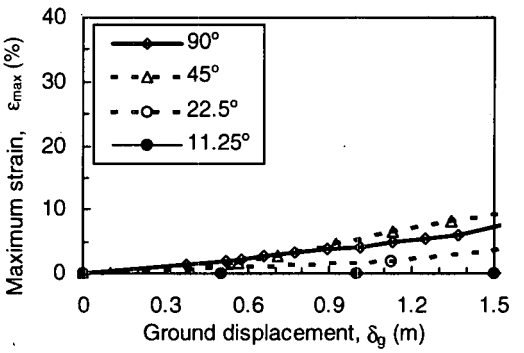

(a) $\psi = 90°-\alpha_i/2$ (opening mode)

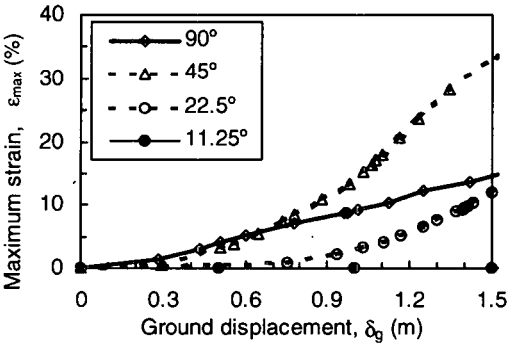

(b) $\psi = 90°+\alpha_i/2$ (closing mode)

Fig. 17 Maximum strain versus ground displacement (300-mm-diameter)

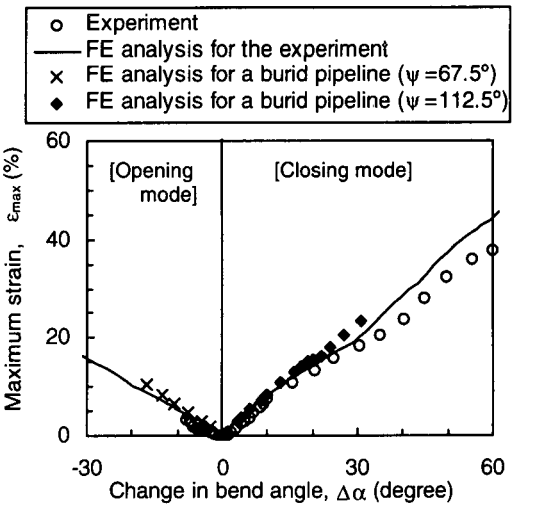

Fig. 18 Comparison in the deformation behavior of the elbow of 300-mm-D with 45° of initial bend angle

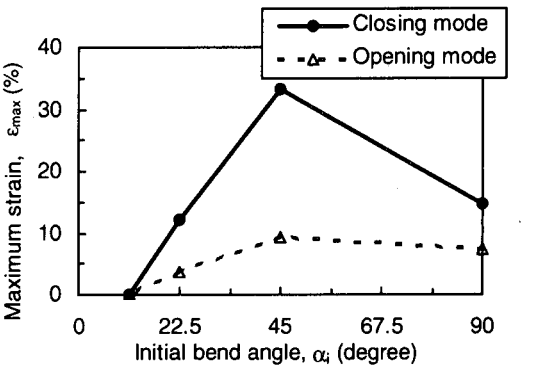

Fig. 19 Maximum strain on the pipelines of 300-mm-D with various kinds of low-angle elbows subjected to 1.5 m of PGD

Earthquake Resistant Design of High Pressure Gas Pipeline"[8)] and data presented by Trautmann and O'Rourke[18)], respectively. **Fig. 16** (a) shows the shear stress vs. relative displacement plot used to model stresses parallel to the pipe longitudinal axis. **Fig. 16** (b) shows the projected stress vs. relative displacement plot used to model stresses normal to the pipe axis. The projected stress acts on an area equivalent to the product of pipe diameter and length to produce the force acting normal to the pipe longitudinal axis. The stresses are generated by discrete spring elements in both the longitudinal and circumferential directions for the shell elements, and in the longitudinal direction for the beam elements, as shown in **Fig. 14** (b).

Fig. 17 shows the analytical results, where maximum strain in either the longitudinal or circumferential direction is plotted vs. ground displacement. The deformation of the elbow is in

the opening mode when ψ equaled to $90°-\alpha_i/2$, and the closing mode when ψ equaled to $90°+\alpha_i/2$, and the results are plotted in **Fig. 17** (a) and (b), respectively.

Fig. 18 compares the FE analytical results of elbow deformation in response to ground displacement with both the experimental measurements and analytical simulations of tests performed on pipeline elbows using the testing device illustrated in **Fig. 1**. The close agreement between analytical and experimental results shows that the deformation behavior of elbows with pipelines subjected to PGD is remarkably consistent with experimental measurements. This similarity in behavior occurs because bending moments are induced by soil-structure interaction in the same way they were simulated in the elbow bending experiments.

Maximum strain is plotted in **Fig. 19** for pipeline elbows of 300-mm diameter, 0.1 MPa internal pressure, and 1.5 m of ground displacement, as a function of the initial bend angle. The analytical results show some noteworthy trends. For example, the largest strains in both the opening and closing modes occur at 45° of initial bend angle. In contrast, **Fig. 6** shows that the largest strains develop in pipe elbows with the smallest initial bend angle in the closing mode, provided that the bending moments required to deflect the elbow to a particular $\Delta\alpha$ have been mobilized. The analyses show that, for this particular cases of 300-mm diameter pipelines, 22.5° and 11.25° of initial bend angle didn't have enough bending moments mobilized by soil-structure interaction to be deflected. The trend shown in **Fig. 19** can be different for pipelines with different diameter, thickness or material. Hence, an accurate simulation of elbow response to PGD depends on both the analytical model for elbows subjected to external loading and the analytical model for soil-structure interaction, pattern and magnitude of PGD, and PGD direction relative to the elbow. With appropriate soil-structure interaction modeling, a rational design process can be developed for the design of new pipelines and the effective rehabilitation of existing ones.

5. CONCLUSIONS

This paper describes in-plane bending experiments that were conducted in the closing and opening mode to evaluate the response of various kinds of low-angle pipeline elbows to earthquake-induced PGD. The following conclusions are drawn in this study:

(1) In the closing mode, no leakage occurred even when both straight pipes connected to the elbows came into contact and measured maximum strain exceeded 70%. The deformation involved ovalization of the elbows. Pipe diameter had little effect on the relationship between maximum strain and bending angle. For the same diameter, elbows with smaller initial bend angles had larger peak values of moment with larger maximum strains for the same change in bend angle.

(2) In contrast, leakage was observed in the opening mode for all cases except the ones that reached the load limit of the hydraulic jack. The strain measured near the crack was 30% in the longitudinal direction. Compared with the closing mode, the maximum changes in bend angle were much smaller in the opening mode. For pipes with the same initial bend angle, elbows subjected to the opening mode with larger diameter experienced larger bending moments, larger maximum strains, and larger % diameter changes for same change in bend angle.

(3) Finite Element (FE) modeling was performed to simulate the deformation behavior of the elbows using linear shell elements. There is very good agreement between the analytical and experimental results for all levels of plastic deformation, including strains as much as 30%.

(4) A modeling technique named HYBRID MODEL was applied for simulating large-scale buried pipelines with low-angle elbows. Analytical results obtained with this model are presented for the behavior of 300-mm-diameter buried pipelines with various kinds of low-angle elbows subjected to PGD. The close agreement between analytical and experimental results show that the modeling procedures result in a simulated elbow deformation that is remarkably consistent with experimental measurements. An accurate simulation of elbow response to PGD depends on both the analytical model for elbows subjected to external loading and the analytical model for soil-structure interaction, pattern and magnitude of PGD, and PGD direction relative to the elbow.

ACKNOWLEDGMENT: The authors wish to thank Mr. Noritake Oguchi, Mr. Takahito Watanabe, Mr. Hirokazu Ando, Mr. Hiroshi Sugawara, Mr. Naoto Hagiwara, Mr. Hiroshi Yatabe and Mr. Naoyuki Hosokawa of Tokyo Gas for their

assistance. This research was conducted using the resources of the Cornell Theory Center, which receives funding from Cornell University, New York State, the National Center for Research Resources at the National Institutes of Health, the National Science Foundation, the Defense Department Modernization Program, the United States Department of Agriculture, and corporate partners. Resources were also provided by the Multidisciplinary Center for Earthquake Engineering Research (MCEER), Buffalo, NY.

REFERENCES

1) Japan Gas Association: *Nihonkai-Chubu earthquake and the city gas*, Japan Gas Association (in Japanese), Tokyo Japan, 1984.
2) O'Rourke, T. D. and Palmer, M. C.: Earthquake Performance of Gas Transmission Pipelines, *Earthquake Spectra*, Vol. 20, No. 3, pp.493-527, 1996.
3) Oka, S.: Damage of Gas Facilities by Great Hanshin Earthquake and Restoration Process", *Proceedings*, 6th Japan-U.S. Workshop on Earthquake Resistant Design of Lifeline Facilities and Countermeasures Against Soil Liquefaction, NCEER-96-0012, MCEER, Buffalo, NY, pp.111-124, 1996.
4) Yoshizaki, K., Hosokawa, N., Ando, H., Oguchi, N., Sogabe, K. and Hamada, M.: Deformation behavior of buried pipelines with elbows subjected to large ground deformation, *Journal of Structural Mechanics and Earthquake Engineering* (in Japanese), JSCE, No. 626/I-48, pp. 173-184. 1999.
5) Yoshizaki, K., Hamada, M. and O'Rourke, T. D.: Large Deformation Behavior of Pipelines with Elbows, *Proceedings*, 5th U.S. Conference on Lifeline Earthquake Engineering, ASCE, Reston, VA, pp. 302-311, 1999.
6) Shima, H., Fujisaki, K. and Kawaguchi, S.: Behavior of bent section of pipeline subjected to large deformation, Proceedings, 45th JSCE Annual Conference, JSCE, Tokyo, Japan, I-577, pp.1184-1185, 1990.
7) Suzuki, N., Katoh, A., Ono, Y. and Yoshikawa, M.: Recent development of seismic design of welded pipelines, NKK report (in Japanese), No. 161, pp.34-38, 1998.
8) Japan Gas Association: *Recommended Practice for Earthquake Resistant Design of Gas Pipeline*, Japan Gas Association (in Japanese), Tokyo, Japan, 1982.
9) ASME: Boiler & Pressure Vessel Code, Section III, Division 1, Subsection NB, 3683.7, 1998.
10) Minami, F., Morikawa, J., Ohmasa, M., Toyoda, M., Konda, N., Arimochi, K., Ishikawa, N., Kubo, T. and Shimanuki, H.: Strength and Fracture Properties of Structural Steels under Dynamic Loading, *Proceedings*, 16th International Conference on Offshore Mechanics and Arctic Engineering, Yokohama, Japan, Vol.3, pp.283-292, 1997.
11) Yoshizaki, K. and Oguchi, N.: Effect of Strain Rate on Stress/Strain Properties of Gas Pipeline Steel, *Proceedings*, 10th Japan Earthquake Engineering Symposium (in Japanese), Yokohama, Japan, pp. 3171-3174, 1998.
12) Goto, Y., Wang, Q., Takahashi, N. and Obata, M.: Three surface cyclic plasticity model for FEM analysis of steel bridge piers subjected to seismic loading, *Journal of Structural Mechanics and Earthquake Engineering* (in Japanese), JSCE, No. 591/I-43, pp. 189-206. 1998.
13) ABAQUS/Standard Theory Manual, ver. 5.8, Hibbit, Karlsson & Sorensen, 1998.
14) ABAQUS/Standard User's Manual, ver. 5.8, vol. 2, Hibbit, Karlsson & Sorensen, 1998.
15) Yoshizaki, K. and Oguchi, N.: Estimation of the deformation behavior of elbows for an earthquake-resistant design, *Proceedings*, 11th World Conference on Earthquake Engineering, Acapulco, Mexico, Paper No. 1783, Elsevier Science, 1996.
16) Hamada, M., Yasuda, S., Isoyama, R. and Emoto, K.: Observations of Permanent Ground Displacements Induced by Soil Liquefaction, *Journal of JSCE* (in Japanese), Tokyo, Japan, No.376, III-6, pp.211-220, 1986.
17) Satoh, M., Isoyama, R., Hamada, M. and Hatakeyama, A.: A procedure to assess the stability of buried structures against liquefaction-induced ground deformations, *Proceedings*, Third International Conference on Recent Advances in Geotechnical Earthquake Engineering and Soil Dynamics, St. Louis, Missouri, Volume 1, pp.221-228, 1995.
18) Trautmann, C. H. and O'Rourke, T. D.: Lateral force-displacement response of buried pipe, *Journal of Geotechnical Engineering*, ASCE, Reston, VA, vol.111 No.9, pp.1077-1092, 1985.

(Received June 26, 2000)

中心角の浅い曲管を有する埋設配管系の大変形特性

吉崎浩司・Thomas D. O'ROURKE・濱田政則

地震時の大規模地盤変位により，埋設配管系の曲管部は大きな変形を受ける可能性がある．本論文では，中心角が45，22.5，11.25度の曲管について面内曲げ実験を実施し，内曲げおよび外曲げ方向の極限状態までの変形特性を明らかにすると共に，シェル要素を用いた有限要素解析がひずみ30%レベルまで有効であることを確認した．更に筆者らの提案した解析モデルにて，中心角の浅い曲管を有する口径300mmの埋設配管系の試解析を実施し，大規模地盤変位に対する中心角と発生ひずみの関係について検討を行った．